AD-A048 014 GENERAL RESEARCH CORP SANTA BARBARA CALIF F/G 4/1
THE ROSCOE MANUAL. VOLUME 10. MODELS OF ION LEAK AND LOSS CONE --ETC(U)
DEC 74 W F CREVIER, R W KILB DNA001-74-C-0182
UNCLASSIFIED DNA-3964F-10 NL

1 OF 1
ADA048014

END
DATE FILMED
1-78
DDC

(12) b.s.

DNA 3964F-10

THE ROSCOE MANUAL

Volume 10 - Models of Ion Leak and Loss Cone Patches

Mission Research Corporation
735 State Street
Santa Barbara, California 93101

16 December 1974

Final Report

CONTRACT No. DNA 001-74-C-0182

THIS WORK SPONSORED BY THE DEFENSE NUCLEAR AGENCY
UNDER RDT&E RMSS CODES B322074464 S99QAXHC06428 AND
B322075464 S99QAXHC06432 H2590D.

Prepared for

Director
DEFENSE NUCLEAR AGENCY
Washington, D. C. 20305

Destroy this report when it is no longer needed. Do not return to sender.

UNCLASSIFIED

SECURITY CLASSIFICATION OF THIS PAGE (When Data Entered)

REPORT DOCUMENTATION PAGE	READ INSTRUCTIONS BEFORE COMPLETING FORM
1. REPORT NUMBER: DNA 3964F-10	2. GOVT ACCESSION NO.
3. RECIPIENT'S CATALOG NUMBER	
4. TITLE (and Subtitle): THE ROSCOE MANUAL, Volume 10, Models of Ion Leak and Loss Cone Patches,	5. TYPE OF REPORT & PERIOD COVERED: Final Report,
6. PERFORMING ORG. REPORT NUMBER: MRC-R-157	
7. AUTHOR(s): W. F. Crevier, R. W. Kilb	8. CONTRACT OR GRANT NUMBER(s): DNA 001-74-C-0182
9. PERFORMING ORGANIZATION NAME AND ADDRESS: Mission Research Corporation, 735 State Street, Santa Barbara, California 93101	10. PROGRAM ELEMENT, PROJECT, TASK AREA & WORK UNIT NUMBERS: Subtasks S99QAXHC064-28 and S99QAXHC064-32
11. CONTROLLING OFFICE NAME AND ADDRESS: Director, Defense Nuclear Agency, Washington, D.C. 20305	12. REPORT DATE: 16 Dec 1974
	13. NUMBER OF PAGES: 38
14. MONITORING AGENCY NAME & ADDRESS (if different from Controlling Office)	15. SECURITY CLASS (of this report): UNCLASSIFIED
	15a. DECLASSIFICATION/DOWNGRADING SCHEDULE

16. DISTRIBUTION STATEMENT (of this Report)

Approved for public release; distribution unlimited.

17. DISTRIBUTION STATEMENT (of the abstract entered in Block 20, if different from Report)

18. SUPPLEMENTARY NOTES

This work sponsored by the Defense Nuclear Agency under RDT&E RMSS Codes B322074464 S99QAXHC06428 and B322075464 S99QAXHC06432 H2590D.

19. KEY WORDS (Continue on reverse side if necessary and identify by block number)

Nuclear Detonation Phenomenology
High Altitude Nuclear Effects

20. ABSTRACT (Continue on reverse side if necessary and identify by block number)

This report presents simple models suitable for use in systems analysis codes of those two of the several possible energy loss mechanisms from high altitude nuclear bursts referred to as the "LOSS CONE" and the "ION LEAK". The "LOSS CONE" represents the escape of debris into the narrow cone of angles parallel to the magnetic field in which the Larmor coupling theory is either inapplicable or partially fails. The "ION LEAK" represents the loss of energy due to ions that at any stage receive a velocity component parallel to the field that is sufficient to allow them to escape along that direction.

DD FORM 1 JAN 73 1473 EDITION OF 1 NOV 65 IS OBSOLETE

UNCLASSIFIED

SECURITY CLASSIFICATION OF THIS PAGE (When Data Entered)

402 754

TABLE OF CONTENTS

RE: Classified References
DNA 3964F-10
Document should remain for unlimited distribution per Ms. Egan, DNA

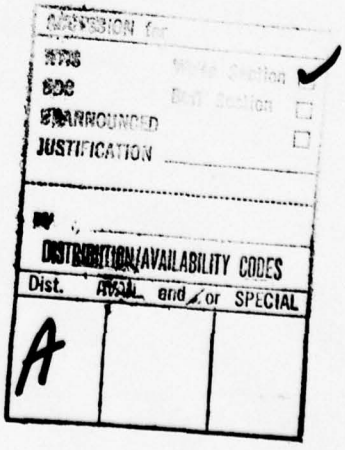

LIST OF FIGURES

SECTION 1

INTRODUCTION

The energy initially in the debris ions of a high altitude nuclear burst can leave the burst region in a variety of ways. This report is concerned with two of these energy loss mechanisms which are referred to as the LOSS CONE and the ION LEAK. The purpose of this report is to present a simple model of these phenomena suitable for use in a systems code such as ROSCOE. Before delving into the details of the models we want to define what we mean by a LOSS CONE and an ION LEAK.

In a high altitude nuclear burst the debris ions can escape the burst region directly with most of their energy (LOSS CONE), or they can give up their energy to air ions some of which may also escape the burst region either as neutrals (CHEX) or as ions (ION LEAK). Another important mechanism for transporting energy away from the burst region is the generation of UV radiation in the shock wave. We are concerned here with modeling the losses due to debris and air ions directly carrying energy from the burst region down (or up) the geomagnetic field lines to the conjugate regions where they stop due to ordinary collisions.

If there were no mechanism for coupling ions, other than ordinary collisions, all the debris ions from a high altitude burst would eventually deposit their energy in the conjugate regions. However, the large electrostatic and inductive electric fields associated with the expansion of the debris ions across the geomagnetic field accelerate air ions and drain energy from the debris ions. These fields can be very effective in coupling together the various ions that are moving perpendicular to the geomagnetic field.

Parallel to the geomagnetic field, however, coupling is weak because the electrons can easily move along the field lines to short out parallel electric fields.

This asymmetry in the coupling makes the behavior of high altitude blast waves quite different than those at lower altitudes where ordinary collisions provide a symmetric coupling mechanism. In particular, one can not assume a fluid like behavior for the ion motion parallel to the magnetic field[1]. Ions can run through other ions without sharing their energy. Wide departures from a Maxwellian velocity distribution can be expected in the parallel direction.

We divide the ions carrying energy directly from the burst region into two separate classes. The separation is somewhat artificial and for some bursts quite arbitrary. However, it lends itself to a simple modeling scheme.

The first class of ions are the debris ions which overrun air ions without losing much of their energy and subsequently escape from the burst region because of the partial failure of the coupling mechanism. The high altitude coupling mechanism we will assume is Larmor coupling, which has been shown to be quite effective over a wide range of burst altitudes and yields. Since Larmor coupling only fails completely in a narrow cone of angles parallel to the ambient geomagnetic field, this loss mechanism is termed the LOSS CONE[2]. This is somewhat of a misnomer however, since much of the loss also comes from debris ions moving in more perpendicular directions. The coupling is much better in these directions but even a small loss over a much larger solid angle can exceed that in the small solid angle where the coupling fails completely.

The debris ions not escaping in the LOSS CONE share their energy with the air ions they overrun, thus setting up a shock wave. The energy in the expanding shock wave is shared by the new air ions being overrun. Some of this energy escapes the shock wave via CHEX,[3,4,5], UV radiation and ION LEAK[6]. The competition between the various loss mechanisms determines what fraction of the coupled kinetic yield comes out in each form[7].

The CHEX loss mechanism involves charge exchange between energetic air ions in the shock and background neutrals. This creates energetic neutral atoms that may escape from the shock zone before being reionized. This CHEX loss is most important in the 200 to 400 km altitude range, especially for smaller bursts.

The UV mechanism involves radiation loss via impact excitation by electrons and ions. It is most effective at altitudes below 200 km.

Although the debris-air and air-air coupling may be very strong transverse to the magnetic field, debris and air ions may still escape from the shock wave if their velocity parallel to the field is sufficiently great. This loss is modeled as the ION LEAK.

The energy loss in the ION LEAK is carried by both debris and air ions. The fraction of the energy carried by each is determined by the amount of air ions in the blast wave at the time this energy escapes. At lower altitudes ($\approx$ 200 km) the vast majority of the ions will be air ions. At very high altitudes ($\approx$ 500 km) there is not much air to mix with and almost all of the debris ions leak out. For very high bursts the distinction between the LOSS CONE and ION LEAK is somewhat academic since the debris energy patch is generated mainly by debris ions escaping directly from the burst region.

For modeling purposes it is convenient to make a distinction between the debris ions which escape because the debris-air coupling is weak (LOSS CONE) and those which escape because there is no coupling in the debris-air shock wave along the magnetic field lines (ION LEAK). For very high altitudes the debris-air coupling is strong in the sense that almost every air ion overrun is picked up, so the LOSS CONE loss is modeled as being small. However, there are so few air ions to pick up that the blast wave is primarily debris ions which eventually leak out to the conjugate regions. Generally, the fraction of the debris ions in the LOSS CONE decrease with altitude while the fraction of the debris ions in the ION LEAK increases with altitude.

In the next section we present the LOSS CONE model. This is followed by Section 3, where the ION LEAK model is developed. Section 4 discusses the parameters that are needed for depositing the energy. The two Appendices give the code listings and input-output information.

SECTION 2

LOSS CONE MODEL

The LOSS CONE model attempts to predict what fraction of the debris kinetic energy will escape directly from the burst region due to failure of debris-air coupling. The model provides as output the total kinetic energy that escapes, the kinetic energy that escapes downward, a characteristic patch radius, and two characteristic velocities.

To guide us in our model making we have the results of several one-dimensional macroparticle debris-air coupling simulations[8,9,10,11,12] and a few two-dimensional Model-5 simulations[13]. Since we need to model a wide range of burst point densities and burst yields, we will base our model on some simple physical principles and then use the macroparticle simulation results to determine the scaling of the parameters that go into the physical equations. This technique gives one a little more confidence about extending the results to yields and altitudes not yet simulated.

The physical model upon which our LOSS CONE model is based makes use of the conservation of canonical momentum. Conservation of canonical momentum provides an algebraic expression for the azimuthal velocity of an ion in terms of the flux surface it was initially on and the flux surface it is currently on:

$$V_\phi = \frac{z_a e}{M_a c\ r \sin\theta}\ (\alpha_o - \alpha). \qquad (2\text{-}1)$$

Here V_ϕ is the azimuthal velocity (in r-θ-ϕ spherical coordinates centered at the burst point, with the polar angle θ measured from the direction of the magnetic field), z_a is the charge state of the air ions, M_a is the mass of an air ion, α_o is the initial flux value of the ion and α is its current value. The flux function is given initially by

$$\alpha_o = \tfrac{1}{2} |B| r^2 \sin^2\theta \tag{2-2}$$

To make use of the algebraic nature of Equation 2-1, we need to make some assumptions about the debris-air interaction. The assumptions we make are fairly good as long as the debris only loses a small fraction of its energy to the air. Fortunately this is the part of the interaction we are interested in modeling. To see what assumptions are appropriate we examine what happens when the leading debris ions expand through the air and across the geomagnetic field. Initially there are

$$N_e = \tfrac{4}{3}\pi n_a z_a r^3 + (N_d)_T z_d \tag{2-3}$$

free electrons inside a sphere of radius r. The factor $(N_d)_T$ is the total number of debris ions and z_d is the average charge of the debris ions. As debris ions stream radially outward the flux surfaces move out so as to enclose the same number of electrons. If N_d debris ions have passed a certain radius, the flux surface now at that radius was initially at a smaller radius given by

$$r_*^3 = r^3 - 3N_d z_d/4\pi n_a z_a \tag{2-4}$$

$$= r^3 - R_b^3$$

where we have defined

$$R_b \equiv (3N_d z_d/4\pi n_a z_a)^{1/3} \tag{2-5}$$

Physically, R_b is the radius of the magnetic bubble boundary after N_d debris ions have streamed out. Inside R_b there is no magnetic field.

Now if we assume that air ions initially at r remain there as the flux surfaces are moved out by the debris ions, we can calculate V_ϕ for the air ions as a function of their radius r:

$$V_\phi = \begin{cases} \tfrac{1}{2}\,\Omega_a \sin\theta\,[r - (1-R_b^3/r^3)^{2/3}] & \text{if } r > R_b \\ \tfrac{1}{2}\, r\,\Omega_a \sin\theta & \text{if } r < R_b \end{cases} \tag{2-6}$$

Here $\Omega_a \equiv Be\, z_a/m_a c$ is the air ion gyrofrequency. The total energy transferred to the air as a function of R_b is

$$E_a(R_b) = \tfrac{1}{2}\,\rho_a \int_0^{2\pi} d\phi \int_0^{\pi} \sin\theta\, d\theta \int_0^{\infty} r^2\, dr\, V_\phi^2 \tag{2-7}$$

$$= \tfrac{1}{4}\pi\rho_a\, \Omega_a^2 \int_0^{\pi} \sin^3\theta\, d\theta \left[\int_{R_b}^{\infty} dr \left[r^2 - (r^3 - R_b^3)^{2/3} \right]^2 + \int_0^{R_b} r^4\, dr \right] \tag{2-8}$$

Doing the r integration we find

$$I = R_b^5 \left[\int_1^{\infty} d\ell \left[\ell^2 - (\ell^3 - 1)^{2/3} \right]^2 + \int_0^1 \ell^4\, d\ell \right]$$

$$I = \beta\, R_b^5 \tag{2-9}$$

where $\beta \approx .707$ and $\ell = r/R_b$.

Thus,

$$E_a(R_b) = \tfrac{1}{4}\,\pi\,\rho_a\,\Omega_a^2\,\beta\int_0^{\pi} R_b^5\,\sin^3\theta\,d\theta. \qquad (2\text{-}10)$$

Now the largest value R_b can have is

$$(R_b)_{max} = (3(N_d)_T/4\pi\,n_a z_a)^{1/3}. \qquad (2\text{-}11)$$

If we set $R_b = (R_b)_{max}$ and integrate over θ we get the same result as Reference 14 except for a small discrepancy in the value of β (they say it should be about 2/3).

However, the approximations used to derive Equation 2-10 generally break down before R_b can reach its maximum value. Note, for example, that there is no yield dependence in the equation. As pointed out in Reference 14, blind aherence to Equation 2-10 can give the result that the air gains more energy than there is in the debris. The problem comes from the assumptions that the air ions remain stationary during the acceleration process. In reality the air ions will begin to move radially outward and the amount of flux moved ahead of the air ions will be less than we have assumed here. Since we are interested in modeling the debris ions which do not couple well we can still use Equation 2-10 if we can find some criteria for limiting R_b to something less than $(R_b)_{max}$.

To estimate what fraction of the debris kinetic energy escapes before the coupling becomes strong, we limit R_b by requiring that the energy the air ions gain from the debris ions which move the bubble boundary from R to $R + dR$ shall not exceed the energy in those debris ions. Since the energy transfer is a function of θ, R_b will also be a function of θ.

Differentiating Equation 2-10 with respect to R and θ gives:

$$\frac{d^2 E_a}{dR_b d\theta} = \frac{5}{4} \pi \rho_a \Omega_a^2 \beta \sin^3 \theta R_b^4 \tag{2-12}$$

for the energy the air in the wedge between θ and $\theta + d\theta$ gains from the debris ions which move the bubble boundary from R to $R + dR$. For a symmetric device, we find that the energy in the debris ions in the same interval is

$$\frac{d^2 E_d}{d\theta\, dR_b} = \pi \sin \theta\, n_a z_a R_b^2 V_d^2 M_b / z_d \tag{2-13}$$

where we have used Equation 2-5 to relate R_b and N_d. V_d is the debris ion velocity which will generally be a function of R_b but which we will treat as a constant.

Equating Equations 2-12 and 2-13 we find that the limiting value of R_b is

$$R_b = \left(\frac{4}{5\Omega_a \Omega_d \beta}\right)^{1/2} \frac{V_d}{\sin \theta} \tag{2-14}$$

where $\Omega_d \equiv Be\, z_d / M_d c$ is the debris ion gyrofrequency. Of course we must limit R_b to be less than its maximum allowed value. If we define

$$R_\perp \equiv \min \begin{cases} \left(\frac{4}{5\Omega_a \Omega_d \beta}\right)^{1/2} V_d \\ (R_b)_{max} \end{cases} \tag{2-15}$$

then when

$$\sin \theta \leq R_\perp / (R_b)_{max} \tag{2-16}$$

we must set R_b equal to $(R_b)_{max}$. Substituting these results into Equation 2-10 gives

$$E_a = \tfrac{1}{2}\,\pi\,\rho_a\,\Omega_a^2\,\beta\left[(R_b)^5_{max}\int_0^{\theta_*}\sin^3\theta\,d\theta + R_\perp^5\int_{\theta_*}^{\pi/2} d\theta/\sin^2\theta\right] \quad (2\text{-}17)$$

where θ_* is the angle for which Equation 2-16 is an equality. Performing the integrations gives

$$E_a = \tfrac{1}{2}\,\pi\,\rho_a\,\Omega_a^2\,\beta\Big[(R_b)^5_{max}[2 - \cos\theta_*(2+\sin^2\theta_*)]/3 + R_\perp^5\cos\theta_*/\sin\theta_*\Big] \quad (2\text{-}18)$$

for the energy transferred to the air by the fast debris ions.

Keep in mind that this is not the total energy transferred to the air but only the energy transferred by the leading debris ions corresponding to R_b values smaller than those given by Equation 2-14. To find the debris energy that escapes we must subtract the energy the air gains from the original energy contained by these leading debris ions.

The energy contained in the leading part of the debris is:

$$E_d = (E_d)_T\left[\int_0^{\theta_*}\sin\theta\,d\theta + \int_{\theta_*}^{\pi/2}\frac{R_\perp^3\,d\theta}{(R_b)^3_{max}\sin^2\theta}\right]. \quad (2\text{-}19)$$

Integrating gives

$$E_d = (E_d)_T\left[(1-\cos\theta_*) + \frac{R_\perp^3}{(R_b)^3_{max}}\,\frac{\cos\theta_*}{\sin\theta_*}\right]. \quad (2\text{-}20)$$

Subtracting Equation 2-18 from 2-20 gives the total energy carried away in the LOSS CONE.

For purposes of analysis it is convenient to define the parameters

$$\epsilon \equiv \frac{4\ V_d^2}{5\ \Omega_a\ \Omega_d\ \beta} \left(\frac{4\pi\ n_a\ z_a}{3(N_d)_T z_d} \right)^{2/3} \tag{2-21}$$

and

$$\epsilon_1 \equiv \min \begin{cases} \epsilon \\ 1 \end{cases} \tag{2-22}$$

Note that when ϵ is less than one $\epsilon_1 = \epsilon$. The parameter ϵ_1 can not exceed one but ϵ can.

We can then write for the energy in the LOSS CONE

$$E_{\ell c} = (E_d)_T \left\{ 1 - (1-\epsilon_1)^{3/2} - [2 - (1-\epsilon_1)^{1/2} (2+\epsilon_1-3\epsilon_1^2)]/5\epsilon \right\} \tag{2-23}$$

where we have used $(E_d)_T = \frac{1}{2} M_d\ (N_d)_T\ V_d^2$ in conjunction with Equation 2-11 to get E_d in terms of $(E_d)_T$.

Figure 2-1 shows a plot of $(E_{\ell c})/(E_d)_T$ as a function of ϵ. When ϵ is small, the energy in the LOSS CONE goes like:

$$E_{\ell c} \approx (E_d)_T\ (3\epsilon/4)\ . \tag{2-24}$$

When ϵ is greater than one $(\epsilon_1 = 1)$

$$E_{\ell c} = (E_d)_T\ [1 - 2/5\epsilon\ ] \tag{2-25}$$

so now the problem is reduced to calculating ϵ for a particular burst.

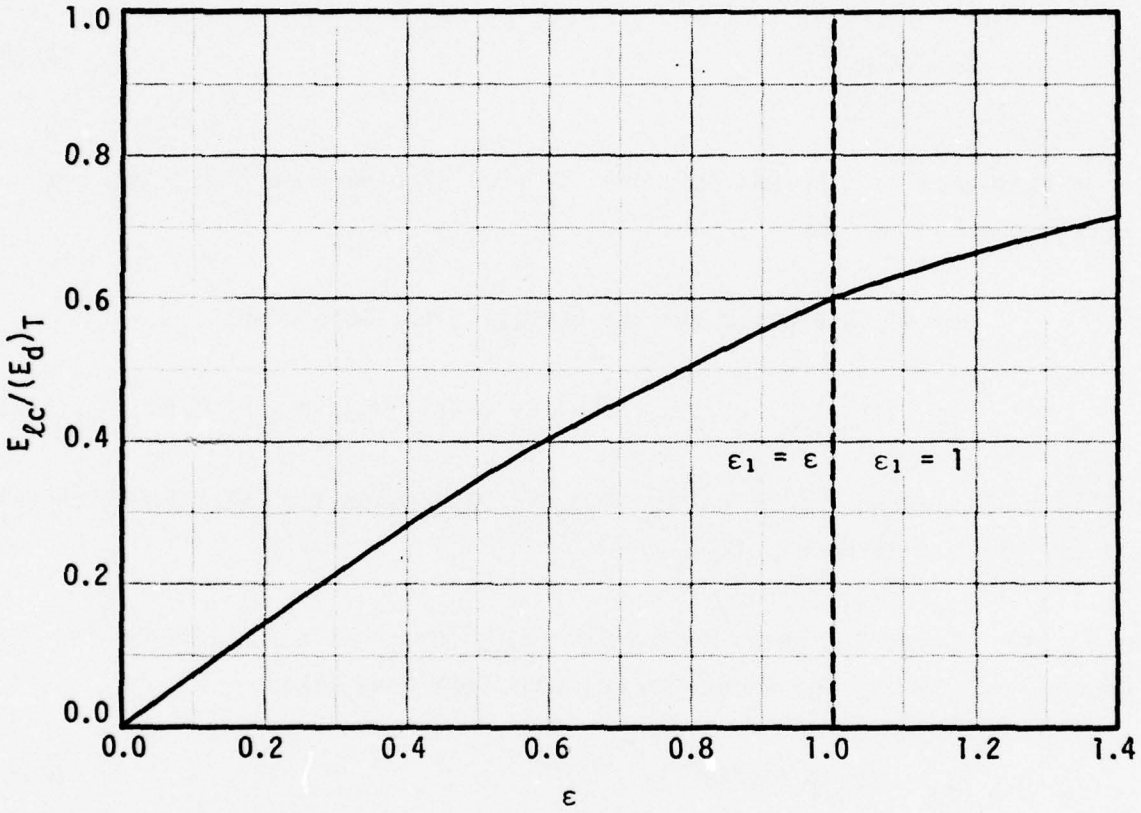

Figure 2.1. Fraction of total debris energy escaping in the loss cone as a function of the dimensionless parameter ε.

Rewriting Equation 2-21 in terms of more fundamental quantities gives

$$\epsilon = \frac{1.4\times10^{-20}}{B^2}\left[\frac{V_d^5\, n_a}{(E_d)_T z_d^{5/2}\, z_a^{1/2}}\right]^{2/3} \qquad (2\text{-}26)$$

Thus, ϵ is a very strong function of such parameters as the debris velocity, the charge states of the debris and air ions, and the geomagnetic field.

The LOSS CONE model needs to provide expressions for V_d, z_d, and z_a in terms of $(E_d)_T$ and n_a that are consistent with the macroparticle debris-air coupling results.

We have fit V_d with

$$V_d = 2.7\times10^8\, W_K^{0.27} \qquad (2\text{-}27)$$

where $W_K \equiv (E_d)_T/4.18\times10^{22}$ is the kinetic yield in MT. We fit the charge state of the air with

$$z_a = \min\begin{cases}7.2\\ 1 + 2.9\times10^{-9}\, V_d\, \ell n[(\rho_a+3\times10^{-15})/3\times10^{-15}]\end{cases} \qquad (2\text{-}28)$$

and

$$z_d = \max\begin{cases}2\\ z_a\end{cases} \qquad (2\text{-}29)$$

These expressions for V_d, z_d, and z_a in terms of $(E_d)_T$ and n_a enable us to calculate ϵ and, through Equation 2-23 the energy in the LOSS CONE for any burst yield and burst point altitude.

Up to this point we have neglected collisions in our LOSS CONE calculations. Equation 2-26 shows that ϵ increases like $n_a^{2/3}$ so at low enough altitudes the LOSS CONE will become very large unless we allow for collisional coupling. Also, even if some debris ions initially escape the burst point there is no point in treating them separately in the ROSCOE code if they deposit their energy within the fireball. Thus, it is clear that we need to reduce the energy in the LOSS CONE by some factor at altitudes where collisions start becoming important.

It is all but impossible to come up with a completely satisfactory simple model for the cut off because of the uncertainties in the environment the escaping debris ions traverse. Because of these uncertainties we have chosen to make the model as simple as possible. The Larmor coupling loss is reduced by the factor

$$f_d = 1-(\rho_a/\rho_d)^2 \quad \text{in the downward direction}$$

and by

$$f_u = 1-(\rho_a/\rho_u)^2 \quad \text{in the upward direction}$$

where ρ_a is the burst point density and ρ_u and ρ_d are chosen to be 2×10^{-11} and 2×10^{-12} corresponding to CIRA mean altitude of about 122 and 151 kms. Note that there is no near conjugate deposition required if ρ_a is greater than ρ_d, but some energy can still escape upwards to the far conjugate as long as ρ_a is less than ρ_u.

These factors are modeled as being independent of yield. Low yield devices have small fireballs but the low velocity of their debris ions makes for efficient atom-atom collisional coupling. High yield devices have larger fireballs but this larger size only partially compensates for the reduction in the atom-atom collision cross section at the higher debris ion velocities. Thus, if there were only atom-atom collisions, large yield devices could be

expected to have a larger percentage of the downward loss cone escape the fireball at any given altitude. We would have to make ρ_d increase with the yield.

However, for these close in depositions, ion-electron collisions may dominate over atom-atom collisions because much of the path will be through highly ionized air. The high charge states associated with the high yield devices will tend to enhance ion-electron collisions for these devices. The uncertainties in the charge states and the electron temperature make a more precise estimate of the collisional coupling impossible. We therefore decided to make the model as simple as possible and did not include a yield dependence.

Figure 2-2 shows the fraction of the debris kinetic energy in the LOSS CONE for various burst altitudes and yields. The burst point densities are taken from the 1965 CIRA mean atmosphere. The 130 km and 150 km curves are significantly reduced from the pure Larmor coupling result due to collisions. The 150 km curve is down about 50% and the 130 km curve is only about 28% of what the pure Larmor coupling result would give.

These results are for a B field of 0.53 gauss which is appropriate for the northern USA. Since ϵ varies like $1/B^2$, the losses will be roughly 3 times higher where the B field is 0.3 gauss. We are a bit nervous about this strong dependence on the geomagnetic field strength but we have never varied the magnetic field strength in the macroparticle debris-air coupling code for a given burst to see how things really scale with B. Since the theory predicts a $1/B^2$ dependence we will use it in our model.

See Section 4 for a discussion of the LOSS CONE patch radius. The velocity spectrum of the escaping debris is also discussed there.

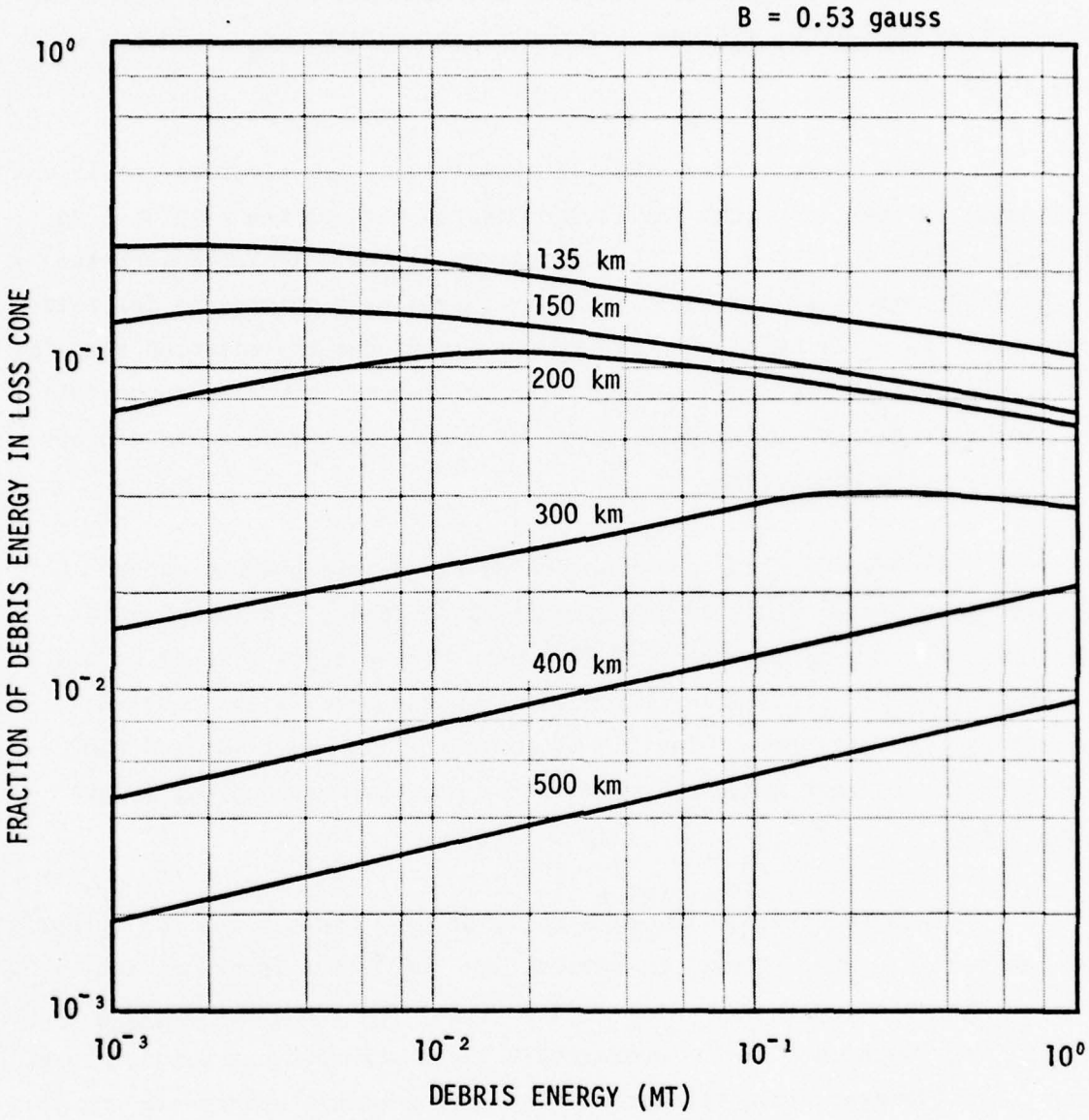

Figure 2-2. Results of the LOSS CONE model for six burst altitudes. A geomagnetic field strength of 0.53 gauss is assumed.

SECTION 3

ION LEAK

While the LOSS CONE is a measure of the failure of debris-air coupling, the ion leak may be considered a measure of the failure of air-air coupling. Once the debris-air coupling proceeds to the point that all the air ions being overrun are picked up, a shock wave is formed. The shock wave is a mixture of debris ions and picked up air ions. It is characterized by an increase in density and by intense fluctuating electric fields which give the ions a fluid-like behavior for motion perpendicular to the distorted geomagnetic field.

These electric fields tend to be weak along the magnetic field so the fastest ions (both debris and air) can leak out of the shock wave and move up and down the geomagnetic field to the conjugate regions[1]. The envelope of the escaping ions has an elliptical shape. The major axis of the ellipse expands up and down the burst point field line with the velocity of the fastest debris ions. The minor axis expands at the shock wave velocity which is somewhat slower because of the picked up air mass. (Actually, the ions exactly along the burst point field line are LOSS CONE ions according to our artificial separation of these two similar phenomena.)

The ION LEAK model attempts to prescribe how much energy escapes from the shock wave as a function of burst point density and burst yield. Since there are currently no codes which simulate the ION LEAK, our model is not as soundly founded as the LOSS CONE model.

The model was formulated on the basis of some general ideas and our best guesses as to how these ideas should be quantified. We would not be surprised if the numbers change considerably as our understanding of the phenomena increases. (In fact, we would be surprised if they did not.) The general ideas upon which the model is based are:

1. We expect that at very high altitudes (greater than 400 km) ION LEAK will be the primary energy loss mechanism, dominating over CHEX and UV losses. We assign a maximum ION LEAK loss of 90%, leaving 10% for the blast wave.
2. At any given very high altitude, low yield devices will leak more energy downward than high yield devices because the downward shock wave from the high yield bursts will extend lower thereby increasing the effectiveness of CHEX.
3. Below about 150 km altitude the downward ION LEAK losses will be effectively zero because the leak particles can not escape the fireball region.
4. Between 150 and 300 km CHEX reduces ION LEAK for low yield devices which can not produce enough ionization near the burst point.

We quantify these ideas with the following equation for the yield in the downward moving ION LEAK:

$$(W_{IL})_d = \frac{0.9}{2} W_1 \left[1 - \left(\frac{\rho_a}{2\times10^{-12} W_1^{1/3}} \right) \frac{1}{25 W_1^{2/5}} \right] \qquad (3\text{-}1)$$

where W_1 is the kinetic yield left after the LOSS CONE energy is removed (in MT) and ρ_a is the burst point mass density.

The upward ION LEAK is not modeled since it is not going to be deposited in the ROSCOE code. Also it is hard to make a distinction between the ION LEAK and the shock wave in the upward direction. We feel that the upward ION LEAK can be adequately treated as part of the upward shock wave.

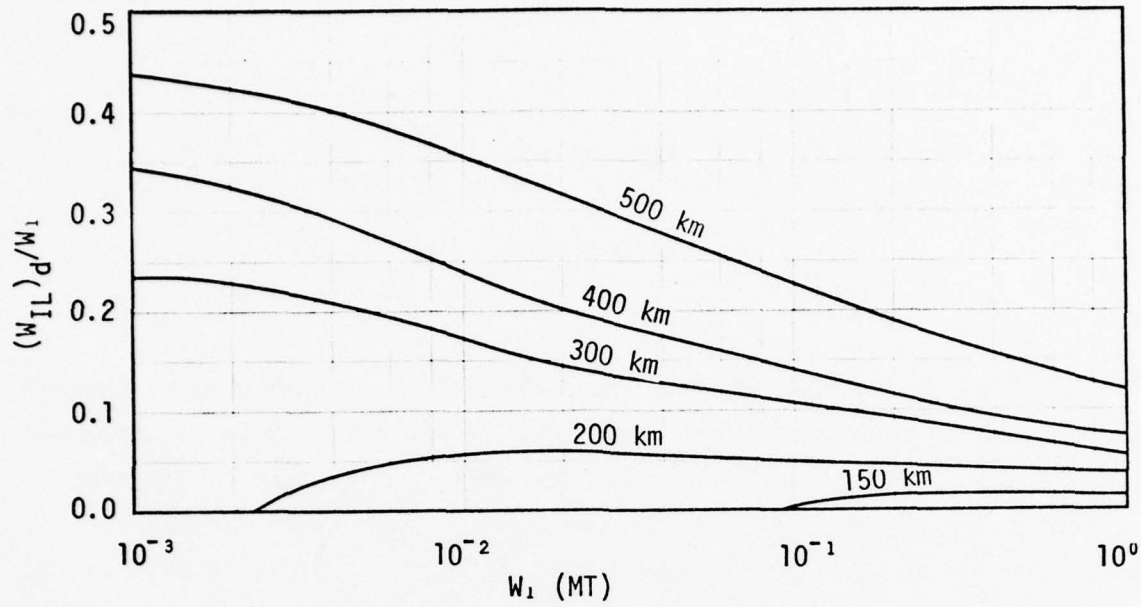

Figure 3-1. Fraction of kinetic yield W_1 (left after the escape of LOSS CONE ions) that escapes in the downward direction via ION LEAK for five burst altitudes.

Figure 3-1 shows how $(W_{IL})_d/W_1$ varies with yield and burst altitude. The densities for each altitude are those from the CIRA 1965 mean atmosphere. Note how at high altitudes the low yield devices leak more than the high yield devices. We have modeled it this way because we believe that the high yield burst's shock wave will extend down to 300 km or lower where charge exchange will become an important loss mechanism. A large fraction of the burst kinetic energy will still be deposited in the conjugate region but a larger fraction of it will be carried there by atoms which escape the burst region as neutrals.

Between 200 and 250 km the ION LEAK loss from the low yield devices drops drastically because much of their energy will be drained away by CHEX neutrals which can successfully compete with ION LEAK at these lower altitudes. The high yield devices' ION LEAK also decreases at lower altitudes, but more slowly. They can ionize such a large volume of air that CHEX can not cut the ION LEAK off as sharply as it can for the low yield devices.

SECTION 4

DEPOSITION

The two previous sections explained how one calculates the amount of energy to be deposited due to the LOSS CONE and ION LEAK losses from the burst region. Before one can deposit this energy a few more things need to be specified. In particular the distribution of the energy in velocity space for each of the two loss mechanisms needs to be specified as does the distribution of the energy on various geomagnetic field lines. This section describes how these are modeled and suggests a possible deposition scheme.

LOSS CONE DEPOSITION

In deriving the LOSS CONE model we made some assumptions about the variation of debris kinetic energy with velocity. The approximations we made are rigorously true only if all the debris ions have the same initial radial velocity V_d where

$$V_d = 2.7\times10^8 \; W_K^{0.27} \quad \text{cm/sec.} \tag{4-1}$$

Here W_K is the burst kinetic energy in MT.

For deposition purposes it is best to have a distribution of velocities. We assume an initial debris distribution of the form

$$\frac{dW_K}{dV} = \frac{5W_K V^4}{V_2^5 - V_1^5} \quad \frac{\text{MT}}{\text{cm/sec}} \quad \text{for} \quad V_1 < V < V_2 \tag{4-2}$$

where

$$V_2 = V_d + 2\times10^7$$

and (4-3)

$$V_1 = \max \begin{cases} 0 \\ V_2 - 4\times10^7 \end{cases}$$

We further assume that the LOSS CONE debris ions have the same distribution but with a reduced energy content $\left[(W_{\ell c})_d \text{ instead of } W_K\right]$. Thus, in the LOSS CONE the energy spectrum is

$$\frac{dW}{dV} = \frac{5(W_{\ell c})_d\, V^4}{V_2^5 - V_1^5} \quad \frac{MT}{cm/sec} \qquad \text{for } V_1 < V < V_2 \,. \tag{4-4}$$

This is easily integrated to give the energy in any velocity interval between V_1 and V_2.

The radius of the LOSS CONE patch is initially only a debris ion Larmor diameter or less. However, this intense concentration of energy causes the air to radiate and the patch grows in size as the radiation ionizes the surrounding air. The ultimate size is determined by factors which limit the radiation transport rather than by the initial deposition.

In any case, the deposition will not be uniform. The intensity will be peaked near the burst point field line and fall off with increasing radius. If we assume that the energy per unit area perpendicular to the geomagnetic field varies like

$$E(r) = \frac{(W_{\ell c})_d}{\pi\, r_0^2\, (1+r^2/r_0^2)^2} \frac{MT}{cm^2} \tag{4-5}$$

we find that the peak energy per unit area is

$$E_p = (W_{\ell c})_d/\pi\, r_0^2. \tag{4-6}$$

See Figure 4-1 for a graph of $E(r)/E_p$.

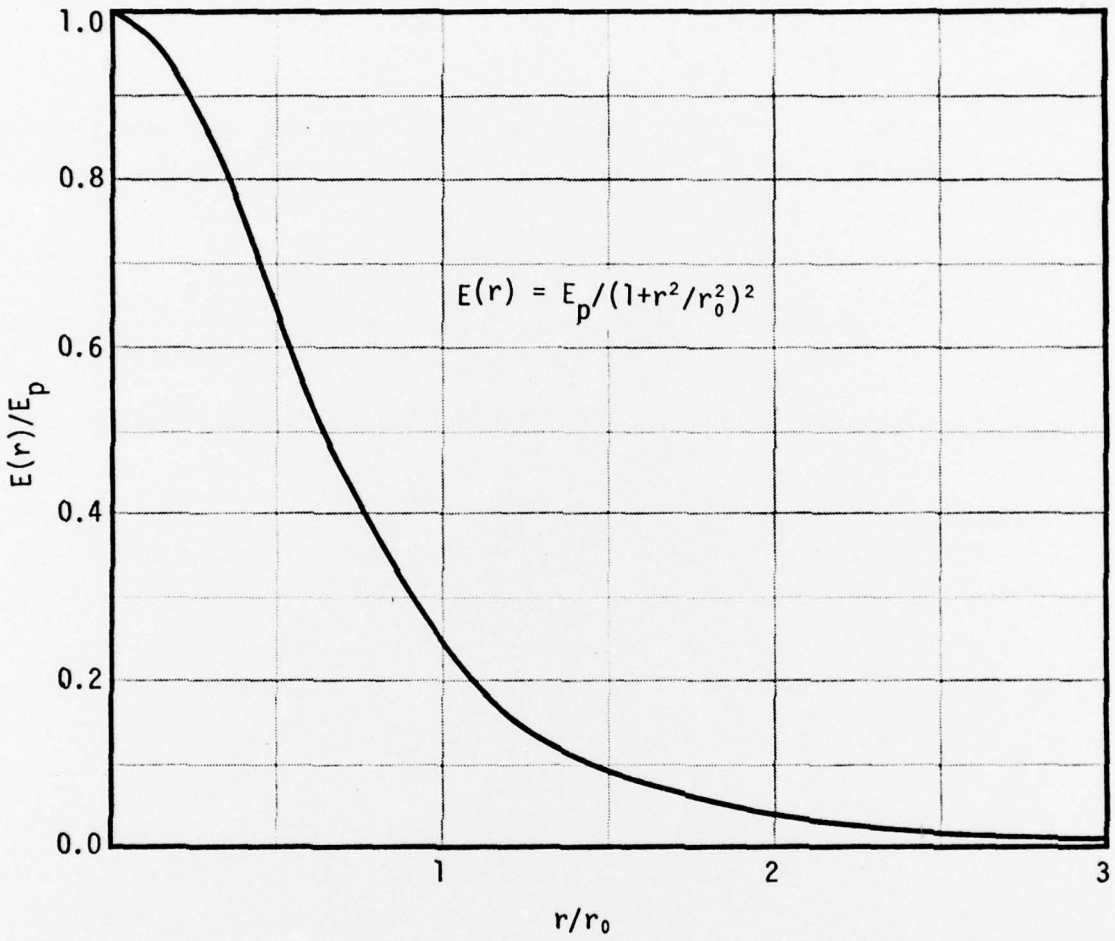

Figure 4-1. The radial dependence of the energy per unit area deposited in the LOSS CONE and ION LEAK patches.

If we assume a stopping range of Range = 8000 $V^{1.8}$ atoms/cm^2 (V in cm/sec)[15] we can estimate how many atoms will share the energy deposited in the column and what average energy each atom will absorb. If we limit the peak absorption to be 8 eV per atom we find

$$(r_0)_{\ell c} = 227 \left[\frac{(W_{\ell c})_d}{V_2^{1.8}}\right]^{1/2} \text{km.} \qquad (4\text{-}7)$$

where $(W_{\ell c})_d$ is the downward LOSS CONE energy in MT and V_2 is in units of 10^8 cm/sec. An absorption of about 8 eV per atom will result in an equilibrium temperature of about 2 3 eV. At this temperature the radiation will be minimal[16].

ION LEAK DEPOSITION

For the ION LEAK patch radius model we were guided by data from the Starfish[17] and Argus III[18] tests. However, the extrapolations to other burst yields and burst altitudes is somewhat arbitrary.

Basically we argued that as the shock wave picked up the ambient air it would begin to slow down. Once its velocity dropped below about 1.5×10^7 cm/sec ordinary collisions would tend to cut the ION LEAK off. So we tried to estimate the radius at which the shock expansion would drop below 1.5×10^7 cm/sec.

The problem is that at high altitudes only the ionized air is picked up so one can not just use the burst point density to estimate the rate of mass pick up in the shock. Also, one must allow for the confining effects of the geomagnetic field at very high altitudes and for the energy that goes into anomalous electron heating[18].

We finally settled upon the following equation for $(r_0)_{IL}$

$$(r_0)_{IL} = 50\left[\frac{10W_1}{\frac{1}{2}B^2 + 2.25\times10^{14}\,\rho}\right]^{1/3} \text{km} \qquad (4\text{-}8)$$

where

$$\rho = \rho_a^2/(\rho_a+8\times10^{-15}). \qquad (4\text{-}9)$$

W_1 is the kinetic energy left after the LOSS CONE energy is removed (in MT), B is the ambient magnetic field in gauss, and ρ_a is the burst point mass density. To get the energy per unit area, we use the same functional form as for the LOSS CONE:

$$(E)_{IL} = \frac{(W_{IL})_d}{\pi\, r_0^2\, (1+r^2/r_0^2)^2}\ \frac{MT}{cm^2} \qquad (4\text{-}10)$$

where r_0 is given by Equation 4-8.

The ION LEAK energy is made up of a mixture of debris and air ions. The velocity spectrum will not be the same as the initial debris velocity spectrum because of all the interactions the ions have undergone before they leak out. We assume they will have a spectrum of the form

$$\frac{dE}{dV} = \frac{E}{V_2 - 1.5\times10^7}\ \frac{MT}{cm/sec} \qquad V_2 \geq V \geq 1.5\times10^7 \qquad (4\text{-}11)$$

where E is given by Equation 4-5 and V_2 is obtained from Equations 4-1 and 4-3.

The ION LEAK model also outputs the amount of debris mass that deposits in the downward direction. The upper limit is taken to be one half

of the total fast debris mass. We expect that this upper limit would be reached at high altitudes where there is very little air to mix with.

At lower altitudes the debris ions give up most of their energy to the air ions so that only a very small amount of debris ions reach the ION LEAK patch. The total fast mass is

$$M_F = \frac{10}{3} W_1 \ (V_2^3 - V_1^3)/(V_2^5 - V_1^5) \times 4.18 \times 10^{22} \text{ gm} \qquad (4\text{-}12)$$

where V_1 and V_2 are output from the LOSS CONE model.

The fraction of this mass deposited in the downward ION LEAK patch is

$$f = \min \left\{ 1/2 \ , \ \frac{(W_{IL})_d \ (V_2^5 - V_1^5) \ \rho_1}{2.5 \times 10^7 \ W_1 \ V_2 \ (V_2^3 - V_1^3)(\rho_1 + \rho_2)} \right\} \qquad (4\text{-}13)$$

where

$$\rho_1 = 2.5 \times 10^{-15} \ B^2 \qquad (4\text{-}14)$$

and

$$\rho_2 = \rho_a^2/(\rho_a + 8 \times 10^{-15}) \ . \qquad (4\text{-}15)$$

DEPOSITION SCHEME

To make use of the quantities modelled above one still needs to have an algorithm for depositing the energy. The basic problem is to calculate for any given point in space the energy per unit area flowing along the geomagnetic field. This flux will depend upon the initial flux and how it has been attenuated between the source point (or points) and the deposition point.

We suggest that the attenuation simply be calculated from the burst point to the point of deposition. This enables one to use the same penetrated mass as is used for the UV depositions. For most geometries the mass calculated this way is within the accuracy for which we know the rate of attenuation.

Equations 4-5 and 4-10 give the initial energy per unit area as a function of r_0, which is modelled, and another radius r. This radius is approximately the horizontal radius from the calculation point to the burst point field line. We say approximately because the divergence of the field lines makes it necessary to specify a single altitude at which the distance between the field lines is measured to ensure that one calculates the same initial flux for all points on the same field line. The altitude specified is not important except that it should be low enough that the burst point field line passes through it. We recommend 100 km altitude.

In summary then, to calculate the energy per unit area perpendicular to the geomagnetic field one first calculates the energy escaping downward in either the LOSS CONE or ION LEAK. One also calculates the appropriate characteristic radius r_0. Then the field line through the calculation point is projected to 100 km altitude and the distance from this point and the intersection of the burst point field line with 100 km is calculated. This length r is used in Equation 4-5 or 4-10 to get E, the energy per unit area starting out on the field line. To get the attenuation between the calculation point and the points where the ions were initially, we recommend that the penetrated mass from the burst point to the calculation point be used. Note that the 100 km altitude is just a reference altitude for calculating r. It has nothing to do with the attenuation.

APPENDIX A

LOSS CONE

INPUT/OUTPUT

The LOSS CONE subroutine (called LOSCONE) requires as input:

1. Burst kinetic yield in megatons
2. Ambient magnetic field at burst point (gauss)
3. Burst point mass density (gm/cm^3)

Additional inputs needed for future refinements might be

4. V_2 - a characteristic velocity
5. ΔV - the velocity spread of the debris energy-velocity distribution
6. z_d - the charge state of the debris
7. z_a - the charge state of the air
8. θ_d - the magnetic dip angle

The code outputs are

1. $W_{\ell c}$ - total energy lost in loss cones (megatons)
2. $(W_{\ell c})_d$ - total energy in near conjugate loss cone patch (megatons)
3. V_2 - the fastest escaping debris ion velocity (cm/sec)
4. V_1 - the slowest escaping debris ion velocity (cm/sec)
5. $(r_0)_{\ell c}$ - characteristic loss cone patch radius (cm)

CODE LISTING

```
      SUBROUTINE LCSCONE(WK,RHOA,BZ,WLC,WLCD,V2,V1,R,DUM)
C  VERSION 2   OCT 31,1974
C  INPUT  WK IN MT,RHOA IN GM/CC, BZ IN GAUSS
C  OUTPUT  WLC AND WLCD IN MT,V2 AND V1 IN CM/SEC, R IN CM
C          DUM IS DUMMY ARRAY FOR FUTURE INPUT/OUTPUT

      DIMENSION DUM(5)
      DATA G,RHOD,RHOU,AIRM/.70738 ,2.E-12,2.E-11,15./
      V=2.7E8*WK**.27
      V2=V+2.E7
      V1=AMAX1(0.,V2-4.E7)
      ZA=1.+AMIN1(6.2,V/3.45E8*ALOG((RHOA+3.E-15)/3.E-15))
      ZD=AMAX1(ZA,2.)
      BNT=2.*WK**4.18E22/(27.*1.66E-24*V*V)
      RXX=(BNT*ZD*.238732*AIRM*1.06E-24/(RHOA*ZA))**(1./3.)
      TIME=SQRT(.8*27.*AIRM/(ZA*ZD*G))/(BZ*9638.554)
      Q=(V*TIME/RXX)**2
      A=AMIN1(1.,Q)
      F=1.-(1.-A)**1.5-3./5./Q*(2./3.-SQRT(1.-A)*((A+2.)/3.-A*A))
      WLCD=F*WK*.5*AMAX1(0.,1.-(RHOA/RHOD)**2)
      WLC=WLCD+F*WK*.5*AMAX1(0.,1.-(RHOA/RHOU)**2)
      R=3.6E14*SQRT(WLCD/V2**1.8)
      RETURN
      END
```

APPENDIX B

ION LEAK

INPUT/OUTPUT

The ION LEAK subroutine (called IONLEAK) requires as input:

1. W_1 - the kinetic yield left after the LOSS CONE losses are subtracted from the initial kinetic yield (MT)
2. B - the ambient geomagnetic field strength at the burst point (gauss)
3. ρ_a - the burst point mass density (gm/cm^3)
4. V_2 - the fastest debris velocity (cm/sec)
5. V_1 - the slowest debris velocity (cm/sec)

The ION LEAK subroutine provides as output:

1. $(W_{IL})_d$ - the yield leaked into the near conjugate (MT)
2. $(r_0)_{IL}$ - characteristic ION LEAK patch radius (cm)
3. M_{IL} - mass of debris ions in near conjugate ION LEAK patch (gm)

CODE LISTING

```
      SUBROUTINE IONLEAK(W1,B,RHOA,V2,V1,WILD,R0,AMIL)
C  VERSION 2 OCT 31,1974
C INPUT      W1 IN MT,B IN GAUSS, RHOA IN GM/CC, V1 AND V2 IN CM/SEC
C  OUTPUT    WILD IN MT,R0 IN CM, AMIL IN GM

      DATA A/.333333333333/
      WILD=AMAX1(0.,.45*W1*(1.-(RHOA/(2.E-12*W1**A))**(.04/W1**.4)))
      IF(WILD.EQ.0.) GO TO 10
      RHOAR=RHOA*RHOA/(RHOA+8.E-15)
      RHOB=2.5E-15*B*B
      R0=.25E7*(10.**W1/(.5*B*B+2.25E14*RHOAR))**A
      GM=V1/V2
      AB=W1*(1.-GM*GM*GM)/(.3*(1.-GM**5)*V2*V2)
      AMIL=AMIN1(.5*AB,2.**WILD/(V2*1.5E7)*RHOB/(RHOB+RHOAR))*4.18E22
      RETURN
   10 AMIL=0.
      R0=0.
      RETURN
      END
```

REFERENCES

1. Longmire, C.L., R.W. Kilb, and W.F. Crevier, The CMHD Approach to High-Altitude Blast Waves (U), DNA3313T (MRC-R-123), Mission Research Corporation, February 1974 (C).

2. Zinn, J., "The Debris Loss Cone (U)", in Proceedings of the High Altitude Nuclear Effects Symposium, Vol. 2, DASA 2455-2, DASIAC, February 1970 (SRD).

3. Hamlin, D.A., R.W. Lowen, and D.H. Sowle, Studies of High Altitude Nuclear Explosion Phenomena (U), DASA 1930, January 1967 (SRD).

4. Workman, J.B., The Charge Exchange Leak (U), DASA 2157, Research Note 792, Avco Everett Research Laboratory, December 1968 (S).

5. Kaufman, A.M. and W.F. Crevier, Studies in Debris Energy Patch Modeling (U), DNA2921F, Mission Research Corporation, December 1973 (U).

6. Fajen, F.E., and D.S. Sappenfield, Single Burst Weapon Effects Calculations for 97-250 km Altitudes (U), LA-4606, Los Alamos Scientific Laboratory, June 1971 (SRD).

7. Tierney, M., and J. Zinn, "The UV-Charge Exchange Energy Loss Partition as a Function of Burst Altitude and Yield-to-Mass Ratio (U)", in Proc. of the DNA 1973 Atmospheric Effects Symposium (U), DNA3131P-8, Defense Nuclear Agency, Summer 1974 (SRD).

8. Kilb, R.W., R.E. Stoeckly, and W.F. Crevier, A Detailed Simulation of Debris-Air Coupling for Spartan at 150 km Altitude (U), MRC-R-142, Mission Research Corporation, September 1974.

9. Kilb, R.W., R.E. Stockely, and W.F. Crevier, Mini-Spartan Macroparticle Simulation at 150 and 200 km (U), DNA3201F (MRC-R-66), Mission Research Corporation, November 1973 (SRD).

10. Kilb, R.W., W.F. Crevier, and F.C. Winter, Detailed Simulation of Debris-Air Coupling for Starfish and Spartan (U), DNA2815F (61TMP-61), General Electric-TEMPO, March 1972 (SRD).

11. Kilb, R.W., and W.F. Crevier, "Detailed Simulation of Checkmate Debris-Air Coupling (U)", published in Proceedings of the DNA High Altitude Nuclear Effects Symposium, DNA2847P-4, December 1972 (SRD).

12. Kilb, R.W., Spartan and Starfish Macroparticle Simulation with Chemistry (U), DASA 2532 (70TMP-50), General Electric-TEMPO, July 1970 (SRD).

13. Crevier, W.F., Two-Dimensional Simulations of Mini-Spartan with Model-5 (U), DNA3200F (MRC-R-69) Mission Research Corporation, December 1973 (SRD).

14. Drummond, W.E., et al., Debris-Air Coupling and Other Plasma Turbulence Effects in High Altitude Nuclear Events (U), DNA2848F (ARA-75), Austin Research Associates, Inc., June 1972 (SRD).

15. Kaufman, A.M., Debris Patch Energy Deposition (U), DNA3215F, Mission Research Corporation, May 1974 (SRD).

16. Sappenfield, D.S., A Study of the Effect of Failure of Short Range Debris-Air Coupling (U), DNA3099T, Mission Research Corporation, June 1973 (SRD).

17. Hoerlin, H., Present Understanding of Starfish (U), LA-4903, Los Alamos Scientific Laboratory, June 1972 (SRD).

18. Kilb, R.W., Analysis of Argus III Photographic Data (U), MRC-R-112, Mission Research Corporation, January 1974 (SRD).

DISTRIBUTION LIST

DEPARTMENT OF DEFENSE

Director
Defense Advanced Research Proj. Agency
ATTN: STO

Defense Communication Engineer Center
ATTN: Code R410, James W. McLean

Director
Defense Communications Agency
ATTN: Code 480

Defense Documentation Center
Cameron Station
12 cy ATTN: TC

Director
Defense Nuclear Agency
ATTN: DDST
ATTN: TISI, Archives
3 cy ATTN: TITL, Tech. Library
ATTN: RAAE

Dir. of Defense Research & Engineering
Department of Defense
ATTN: S&SS (OS)

Commander
Field Command
Defense Nuclear Agency
ATTN: FCPR

Director
Interservice Nuclear Weapons School
ATTN: Document Control

Director
Joint Strat. Target Planning Staff, JCS
ATTN: JPST, Captain G. D. Goetz

Chief
Livermore Division, Field Command, DNA
Lawrence Livermore Laboratory
ATTN: FCPRL

DEPARTMENT OF THE ARMY

Commander/Director
Atmospheric Sciences Laboratory
US Army Electronics Command
ATTN: DRSEL-BL-SY-S, F. E. Niles

Director
BMD Advanced Tech. Center
Huntsville Office
2 cy ATTN: ATC-T, Melvin T. Capps

Commander
Harry Diamond Laboratories
ATTN: DRXDO-NP, Francis N. Wimenitz
ATTN: DRXDO-TI

Director
TRASANA
ATTN: R. E. DeKinder, Jr.

DEPARTMENT OF THE ARMY (Continued)

Director
US Army Ballistic Research Labs.
ATTN: Lawrence J. Puckett
ATTN: Mark D. Kregel

Commander
US Army Foreign Science & Tech. Center
ATTN: P. A. Crowley

Commander
US Army Missile Intelligence Agency
ATTN: Jim Gamble

Commander
US Army Missile Command
ATTN: DRSMI-XS, Chief Scientist

Commander
US Army Nuclear Agency
ATTN: MONA-WE, J. Berberet

DEPARTMENT OF THE NAVY

Chief of Naval Operations
Navy Department
ATTN: Alexander Brandt

Commander
Naval Ocean Systems Center
3 cy ATTN: Code 2200, Verne E. Hildebrand

Director
Naval Research Laboratory
3 cy ATTN: Code 7701, Jack D. Brown
ATTN: Code 7750, S. Ossakow

Commander
Naval Surface Weapons Center
ATTN: Code WA501, Navy Nuc. Prgms. Off.
ATTN: Code WX21, Tech. Lib.

Director
Strategic Systems Project Office
Navy Department
ATTN: NSP-2722, Marcus Meserole
ATTN: NSSP-2722, Fred Wimberly

DEPARTMENT OF THE AIR FORCE

AF Geophysics Laboratory, AFSC
ATTN: OPR, James C. Ulwick
ATTN: OPR, Alva T. Stair
ATTN: OPR, Harold Gardner

AF Weapons Laboratory, AFSC
ATTN: NSS, John M. Kamm
ATTN: SUL
ATTN: DYT, Captain Mark A. Fry
ATTN: DYT, Captain L. Wittwer
ATTN: DYT, Peter W. Lunn

Hq. USAF/RD
ATTN: RDQSM

DEPARTMENT OF THE AIR FORCE (Continued)

Commander
Rome Air Development Center, AFSC
ATTN: EMTLD, Doc. Library

SAMSO/SZ
ATTN: SZJ, Major Lawrence Doan

Commander in Chief
Strategic Air Command
ATTN: ADWATE, Captain Bruce Bauer
ATTN: XPFS, Major Brian G. Stephan

Hq. USAF/SA
ATTN: AFSA, Captain Henkle

ENERGY RESEARCH & DEVELOPMENT ADMINISTRATION

University of California
Lawrence Livermore Laboratory
ATTN: Ralph S. Hager, L-31
ATTN: Donald R. Dunn, L-156

Los Alamos Scientific Laboratory
ATTN: Doc. Con. for John Zinn
ATTN: Doc. Con. for Eric Jones

OTHER GOVERNMENT AGENCIES

Department of Commerce
Office of Telecommunications
Institute for Telecom Science
ATTN: William F. Utlaut

DEPARTMENT OF DEFENSE CONTRACTORS

Aerospace Corporation
ATTN: Norman D. Stockwell
ATTN: Doug Rawcliffe

Brown Engineering Company, Inc.
ATTN: James E. Cato
ATTN: Romeo DeLiberis
ATTN: Joel D. Bigley

ESL, Inc.
ATTN: James Marshall
ATTN: C. Prettie

General Electric Company
TEMPO-Center for Advanced Studies
ATTN: Warren S. Knapp
ATTN: Tim Stephens
ATTN: DASIAC

General Research Corporation
ATTN: John Ise, Jr.
ATTN: Joel Garbarino

DEPARTMENT OF DEFENSE CONTRACTORS (Continued)

Jaycor
ATTN: S. R. Goldman

Johns Hopkins University
Applied Physics Laboratory
ATTN: Document Librarian

Lockheed Missiles & Space Company, Inc.
ATTN: D. R. Churchill

M.I.T. Lincoln Laboratory
ATTN: Lib. A-082 for David M. Towle

Martin Marietta Aerospace
Orlando Division
ATTN: Roy W. Heffner

Mission Research Corporation
ATTN: D. Sappenfield
ATTN: R. Bogusch
ATTN: R. Hendrick
ATTN: Russell Christian
ATTN: W. F. Crevier
ATTN: R. W. Kilb
ATTN: A. H. Michelet

Physical Dynamics, Inc.
ATTN: Joseph B. Workman

R & D Associates
ATTN: Bryan Gabbard
ATTN: Robert E. LeLevier

Science Applications, Inc.
ATTN: D. Sachs
ATTN: Curtis A. Smith
ATTN: Daniel A. Hamlin
ATTN: Robert W. Lowen
ATTN: Melvin R. Schoonover

Science Applications, Inc.
Huntsville Division
ATTN: Dale H. Divis
ATTN: Noel R. Byrn

Stanford Research Institute
ATTN: Walter G. Chestnut

VisiDyne, Inc.
ATTN: J. W. Carpenter
ATTN: Charles Humphrey